

# Neural NDT by means of Reflected Longitudinal and Torsional Waves Modes in Long and Inaccessible Pipes

BARBARA CANNAS, FRANCESCA CAU, ALESSANDRA FANNI, AUGUSTO MONTISCI, PIETRO TESTONI,  
MARIANGELA USAI  
Electrical and Electronic Engineering Department.  
University of Cagliari.  
Piazza D'Armi.  
ITALY.

*Abstract:* - The design of Non-Destructive Testing systems for fault detection in long and not accessible pipelines is an actual task in the industrial and civil environment. At this purpose the diagnosis based on the propagation of guided ultrasonic waves along the pipes offers an attractive solution for the fault identification and classification. The authors studied this problem by means of suitable Artificial Neural Network models. Numerical techniques have been used to model different kinds of pipes and faults, and to obtain several returning echoes containing the fault information. Two kinds of excitation waves have been used: longitudinal and torsional wave modes. The obtained signals have been processed in order to filter the noise, to reduce the data dimensionality, and to compute suitable features. The features selected from the signals can be further processed in order to limit the size of the Neural Network models without loss of information. At this purpose, the Principal Component Analysis has been investigated. Finally, the selected features have been used as input for the Neural Network models. In this paper, traditional feed-forward, Multi Layer Perceptron networks have been used to classify position, width, and depth of the defects.

*Key-Words:* - Non-Destructive Testing, Finite Element Analysis, Neural Network, Blind Separation, PCA.

## 1 Introduction

The presence of flaws and corrosion in pipes is one of the major problems in industrial and civil plants, as water, oil, steam, and gas pipelines. The Non-Destructive Testing (NDT) with ultrasonic guided waves in the pipe wall provides an interesting solution to the fault inspection problem because it allows to inspect long pipes, positioning a ring transducer in only one point, usually accessible for inspections, without dismantling and interrupting the service, favoring the least uneasiness and economic loss [1] [2]. At this purpose, particular ultrasonic guided waves, called Lamb Waves [3], can be excited at the edge of the pipe and will propagate many meters, returning echoes indicating the presence of faults, such as corrosion, cracks, etc.

In this work, several testings have been performed using longitudinal and torsional wave excitations. In contrast to longitudinal mode, the torsional mode propagation characteristics are not affected by the presence of fluid in the pipes and there is no other axisymmetric torsional mode in the frequency range. However, providing suitable preprocessing, both the excitations permit to obtain comparable results.

The diagnostic system proposed in this paper is based on Artificial Neural Networks (NNs), for their ability of generalization and for the characteristic of not requiring any fault physical

model. In particular, fault diagnosis has been modeled as a pattern recognition process in which the classifier is a neural network. Classically, a pattern recognition system is composed of three modules [4]: a transducer that acquires data on a physical device; a feature extractor, whose purpose is to reduce the data dimensionality that the transducer produces, to filter the noise, and to compute significant features or properties; a classifier that makes a decision on the class whose the fault belongs to.

In the diagnostic system we propose in this paper, the transducer is made up of mechanically independent dry-coupled piezo-electric elements distributed around a circumference; the feature extractor may be Wavelets, Blind Separation, Fast Fourier Transform (FFT), Principal Component Analysis (PCA), or other statistics based on time or frequency analysis; the classifier is a Multi Layer Perceptron (MLP) neural network.

Two main phases can be recognized in the diagnostic task: the training phase and the defect detection phase. During defect detection operations, the signals acquired on the actual pipe have to be preprocessed and used as inputs to the neural network that has been previously trained using a numerical model of the pipe. This choice decreases the developing time and permits to automatically create the training, validation and test sets needed to build the neural network

Deleted: of

diagnostic system. Theoretically, it may be possible to use actual measurements in the training phase, but this is not practical. In fact, the data to feed the NNs during the training phase are the waves reflected by the defects. These signals can be obtained by a large amount of experimental tests, which consist in building artificially several faults of different dimension and position in a certain number of pipes. This process is very expensive, complex and time consuming, especially if various and numerous datasets are required. Thus, the alternative way consists of obtaining the required signals by using numerical analysis, e.g., the Finite Element Method (FEM) [5]. Also in this case the data will be few numerous and will have a large dimensionality. In fact, the solution of the numerical models requires a large amount of memory space and CPU time, as the pipelines to be studied are several meters long and many features characterize each signal. However, real acquisitions can be used in particular cases, e.g., to estimate the magnitude of the measurement noise.

The use of a finite element code can substitute the experimental tests, providing signals, which are as close as possible to the real data.

In this paper, two kinds of excitation have been examined:

- Longitudinal wave mode.
- Torsional wave mode.

In a first task, several pipes with different defects have been modeled and a longitudinal mode has been used as excitation signal. A sensitivity analysis has been performed to set up the model that guarantees to obtain signals with the highest informative content.

The obtained synthetic signals have been preprocessed with Discrete Wavelet Transform (DWT) [6] and Blind Separation techniques [7] to filter the noise, and then passed to a feature extraction system in order to reduce the data dimensionality.

The number of the features has been further reduced by using the Principal Component Analysis.

In a second task, further analysis has been done by using a torsional mode as excitation signal. In this case, the resort to the DWT and Blind Separation was unnecessary, because the mode shape of the torsional mode is not frequency dependent and it is completely non dispersive. In fact, as specified in [8], no other torsional mode is present in the used frequency range for both finite element models and experiments. The database

which refers to the torsional waves has been provided by the research group of the University of Pisa and it has been achieved by using the commercial simulation code CAPA [9]. PCA and Fast Fourier Transform (FFT) have been used to preprocess the signals and to obtain the features to feed the neural network models.

In particular, Multi Layer Perceptron (MLP) networks have been used to act as pattern classifiers, trained by using back-propagation learning with Levenberg-Marquard rule. This choice is corroborated by most of the literature, as reviewed in [10]. Basically, the main feature of a MLP resides in its intrinsic ability to perform extremely complex tasks in a very short time, once the learning phase ends. The networks have as many nodes in the input layer as the number of significant features extracted from the signals, while the number of output nodes depends on the fault coding chosen by the designer. In this paper different codings are tested to code the different geometrical parameters characterizing the faults.

## 2 Neural Network Architecture

The use of non-conventional approaches for NDT, such as neural networks, is justified by the difficulty of finding a proper solution to this problem by using standard methods. The most widely used neural classifier is the Multi-Layer Perceptron (MLP). A MLP neural network is constituted by an input layer, one or more hidden layers, and one output layer of neurons. The neurons of each layer are connected with all the neurons of the previous layer. The connection weights are the free parameters of a learning process. They are determined by presenting to the network a set of actual input-output values (the training set).

During the learning process the network output and the desired output are compared through the error function. To evaluate the network performances the trained network is applied to a new set of examples (the test set).

It can be noted that, if the number of examples in the training set is limited, as in the present problem, the network size (i.e., the number of connection weights) has to be limited, in order to avoid the overfitting of the network. This can be done by limiting the number of hidden layers, or the number of neurons in the hidden layers, or reducing the number of input neurons.

In the present paper, an MLP with one hidden layer has been chosen. As in the most of applications presented in literature, the size of hidden layer has to be heuristically determined.

Deleted: be

Deleted: to

Deleted: has been

Deleted:

Deleted: overcome

Deleted: single layer

Deleted: part

In particular, the growing method has been adopted. It consists on training a network having few neurons and then evaluating their performance. If such performance is satisfactory, the procedure ends, otherwise a new network having more hidden neuron is trained, and so on, until the network reaches the desired performance. In this way the training procedure avoids the overfitting, which derives from the excessive number of degrees of freedom.

The overfitting can derive also by the overtraining. In order to avoid this problem, a set of examples, called validation set, is left out of the training set. During the training phase, the mean square error, evaluated on the validation set, gives us information regarding the overtraining. As the error on the validation set begins to rise, the training process terminates (early stopping).

To increase the resolution power of the model, limiting, at the same time, the number of input neurons, feature extraction and data reduction strategies have been adopted, as described in the following.

### 3 Longitudinal Wave Mode

In the following, a detailed description of the bidimensional model used to generate our synthetic data is reported. Data have been generated by simulating axisymmetric defects using the commercial finite element code ANSYS [11].

The theory of the elastic wave propagation in a hollow cylinder is based on the Navier's equations of motion in a cylindrical coordinate system [12]:

$$\mu \nabla^2 \mathbf{u} + (\lambda + \mu) \nabla (\nabla \cdot \mathbf{u}) = \rho \frac{\partial^2 \mathbf{u}}{\partial t^2} \quad (1)$$

with

$$\lambda = \frac{\nu E}{(1 + \nu)(1 - 2\nu)} \quad (2)$$

and

$$\mu = \frac{E}{2(1 + \nu)} \quad (3)$$

where  $\mathbf{u}$  is the displacement field,  $E$  is the Young modulus of the material,  $\nu$  is its Poisson's modulus,  $\rho$  is its density and  $\lambda$  and  $\mu$  are its Lamè constants, determined by (2) and (3).

The differential equation (1) can be solved in boundary problems through a numerical approach.

Finite element axisymmetric models have been built in order to simulate the wave propagation in the pipes. A mesh of identical quadrilateral linear elements with four nodes has been used. The structural module of the code ANSYS solves the (1) by applying the principle of the virtual works.

This principle states that, by imposing a system of "virtual" displacements (small and compatible with the constraints) and by keeping constant the internal strains and the external forces, the comprehensive "virtual" work is equal to zero. Namely, the external applied loads make a work equal to that made by the internal strains. This can be mathematically expressed by the following (4):

$$\delta U = \delta V \quad (4)$$

where  $U$  and  $V$  are the internal and the external work respectively, while  $\delta$  is the virtual operator. By following the analytical procedure described in [13] and expressing the term  $\delta U$  and  $\delta V$  as a function of the strains  $\sigma$  and the deformations  $\epsilon$ , the following is found:

$$[\mathbf{K}_e] \mathbf{u} - \mathbf{F}_e^{th} = [\mathbf{M}_e] \ddot{\mathbf{u}} + \mathbf{F}_e^{pr} + \mathbf{F}_e^{nd} \quad (5)$$

where  $[\mathbf{K}_e]$  is the element stiffness matrix which depends on the geometry and on the material properties of the used elements;  $\mathbf{u}$  is the nodal displacement vector;  $[\mathbf{M}_e]$  is the element mass matrix and  $\ddot{\mathbf{u}}$  is the acceleration vector;  $\mathbf{F}_e^{th}$  represents the element thermal vector load,  $\mathbf{F}_e^{pr}$  is the element pressure vector and  $\mathbf{F}_e^{nd}$  is the vector that represents the nodal forces applied to the element. By assembling the terms that represent the external loads, the (5) can be simply written:

$$[\mathbf{M}] \ddot{\mathbf{u}} + [\mathbf{K}] \mathbf{u} = \mathbf{F}^A \quad (6)$$

where  $[\mathbf{M}]$  is the structural mass matrix,  $[\mathbf{K}]$  is the structural stiffness matrix and  $\mathbf{F}^A$  is the applied load vector. The Newmark time integration method [14] has been used for the solution of the (6). This method uses finite difference expansions in the time interval  $\Delta t$ , in which it is assumed that:

$$\dot{\mathbf{u}}_{n+1} = \dot{\mathbf{u}}_n + ((1 - \delta) \ddot{\mathbf{u}}_n + \delta \ddot{\mathbf{u}}_{n+1}) \Delta t \quad (7)$$

and

$$\mathbf{u}_{n+1} = \mathbf{u}_n + \dot{\mathbf{u}}_n \Delta t + \left( \left( \frac{1}{2} - \alpha \right) \ddot{\mathbf{u}}_n + \alpha \ddot{\mathbf{u}}_{n+1} \right) \Delta t^2 \quad (8)$$

Deleted: one

Deleted: (5)

Deleted: which

Deleted: :

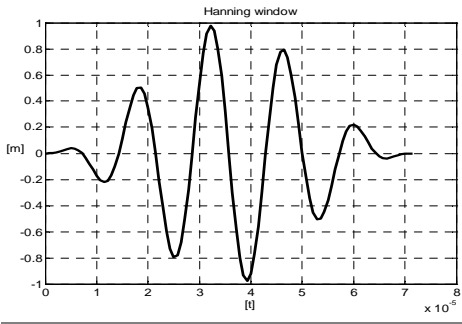


Fig. 1. Exciting waveform signal

where  $\alpha$  and  $\delta$  are the Newmark integration parameters. By choosing  $\delta=1/2$  and  $\alpha=1/4$  the system is stable [5] and can be integrated.

The key problem associated with the measurement of the propagating Lamb waves characteristics is that more than one mode can exist at any given frequency. In NDT inspection system, selection and exploitation of a single mode is very important. In fact, generally, an excitation source can excite all the modes, which exist within its frequency bandwidth, resulting in a signal, which is much too complicated to interpret. Even with a single mode, great care is needed for correct identification of the echoes reflected by the defects and by normal pipe features such as welds. So, it is essential to design the transducers and to choose the forcing signal in order to excite only the chosen mode. In fact, theoretical and experimental results show that suitable mode and frequency can be chosen to produce a better penetration power and good results. In this paper, the axial (or longitudinal) symmetric mode at 70 kHz has been chosen according to bibliography [1]. This mode is very attractive for testing for several reasons:

- it is practically non-dispersive over a wide bandwidth around this frequency (its velocity does not vary significantly with frequency), so that the signal shape and amplitude are retained as it travels;
- it is the fastest mode so that any unwanted mode converted signal arrives after it has been received;
- its mode shape makes it equally sensitive to internal or external defects at any circumferential location.

Thus, an excitation tone burst with a narrow band has been selected, in order to obtain good signal strength and to avoid dispersion over long propagation distances. The excitation is a force signal applied in the extremity node of the model,

it is a five-cycle tone burst enclosed in a Hanning window as described by (9) and reported in Fig.1 [15]:

$$y = \sin(2\pi ft) \sin\left(\frac{2\pi ft}{10}\right)^2 \quad (9)$$

The parameter  $f$  is the excitation frequency chosen by the previous considerations. The Hanning windowing is largely used to reduce the leakage, which occurs when the signals are not periodic in the temporal and spatial sampling window. The aliasing has been avoided by sampling the data with a suitable high frequency.

In the examined cases, the piezo-electric transducer has been simulated as made up of mechanically independent dry-coupled elements distributed around a circumference, located at the edge of the pipe. The generated wave propagates in the pipe walls until it is reflected by a defect or a discontinuity. The returning echo is received by the same excitation transducer, which also works as a survey probe.

A test pipe has been considered. It has been represented by an axisymmetric model; the mesh has been built throughout identical four nodes quadrilateral linear elements (PLANE 42 in Ansys). The model dimension and the material properties are listed in Table 1.

A sensitivity analysis of the pipe model without defects has been performed. The purpose of this test is to set the simulation parameters, i.e., the dimensions of the elements in the FEM model, and the sampling time (see Table 2). Decreasing the sampling time (or the element length) the precision of the results increases, on the other hand, the simulation process time increases. A compromise has to be found between these contrasting requirements. The sampling time identifies the instants in which the solution is calculated; moreover a sub-sampling has been done, namely only one sample data every two has been stored; in fact, this operation allows reducing the storage memory, preserving the informative content of the signals.

Table 1: Geometric dimensions and material properties of the modelled pipe

Length of the pipe	15 m
Outer radius	0.11 m
Thickness	0.005 m
Young's modulus	219 GN/m <sup>2</sup>
Poisson's coefficient	0.286
Density	8000 kg/m <sup>3</sup>

Deleted: identify

Deleted: s

Deleted: Dimensions

Deleted: Material

Deleted: Properties

Deleted: Modelled

Deleted: Pipe

Deleted: T

**Table 2: Element dimensions and sampling time**

Element length [mm]	3
Number of axial subdivisions	5000
Number of radial subdivisions	5
Sampling time [ms]	1/700

**3.1 Fault diagnosis**

The second part of the numerical study concerns the simulation of a pipe with a notch in the external wall. Varying the position and the dimension of the defect several simulations has been performed. In order to reduce data to be stored, the returned echo has been surveyed only during prefixed time windows. The fault position have been varied within the range [0.5\_m ÷ 7 m], with a step of 0.5 m. For each position the notch width and depth have been varied as reported in Table 3. The resulting data set is composed by 100 signals, which are divided in two sets: the training set is composed by 86 signals, and the test set is composed by the remaining 14 signals. The limited number of simulations is due to the high CPU time needed for each of them.

**3.2 Preprocessing**

The reflected waveform is deformed, if compared with the exciting one, due to both the defect and the residual oscillations in the pipe. The DWT [16] and the Blind Separation [17] techniques have been used to denoise this reflected wave. In fact, the reflected signal is the sum of two contributes, one due to the fault, and one due to a residual oscillation at the resonance frequency of the structure. This residual wave is characterized by some low-frequencies components, which do not provide any information about the defect.

The DWT allows removing this second component of the signal, performing a multilevel decomposition in approximations and details.

The approximations are the high-scale, low-frequency components of the signal, while the details are the low-scale, high-frequency

**Table 3: Geometric fault characteristics**

	Range	Step
Position [m]	0.5-7	0.5
Depth [mm]	1-4	1
Width [mm]	12-30	6

components. The decomposition of the signal into different frequency bands is simply obtained by successive high-pass and low-pass filtering of the time domain signal.

In the present paper, each waveform achieved by the finite element simulation has been decomposed in three levels by using the DWT technique; then the details components at high frequency have been reconstructed to obtain the reflected wave due only to the fault in the modelled pipe.

In fact, in most cases, the signal received by a sensor is the sum of a certain number of elementary contributions named sources. These sources are usually unknown, and a separation of sources is needed.

In this paper, a blind identification procedure is used to extract the different sources received by the sensor, by using an adaptive system, the SOBI (Second Order Blind Identification) algorithm, available on the ICALAB Package for Signal Processing Toolbox of Matlab [18].

Results obtained by using the DWT and Blind Separation are very similar. Fig. 2 represents an example of signal before and after the preprocessing phase, performed by SOBI.

**3.3 Features extraction**

Different features have been considered in order to reduce filtered signal dimensionality. The feature extraction method is based on both time and frequency analysis. The choice of the feature extraction technique depends on the fault characteristics. The selected features have been chosen according to literature [19]. In particular, 39 features are calculated in the time domain and 7

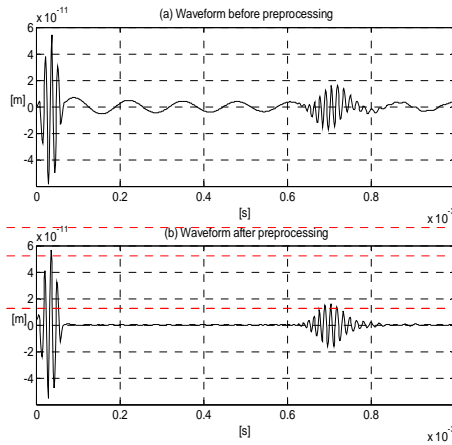


**Fig. 2. Signal before (a) and after (b) preprocessing phase**

Deleted: Dimensions

Deleted: Sampling

Deleted: Time

Deleted: has

Deleted: to

Deleted: Discrete Wavelet Transform (

Deleted: )

Deleted:

Deleted: low

Deleted: Fault

Deleted: Characteristics

in the frequency domain. All these features present significant variations for the 100 simulations considered.

### 3.4 Data Reduction

As previously highlighted, the number of significant features suggested by the literature is too large, compared to the limited number of available simulations. Thus, different methods of data reduction have been tested. The best results are obtained using the PCA.

This method consists of orthogonalizing the components of the input data in such a way that they are uncorrelated one to each other, ordering the resulting orthogonal components (principal components) and finally eliminating those that contribute the least to the variation in the data set. The Signal Processing Toolbox of MatlabR12 has been used. This routine employs singular value decomposition to compute the principal components [13].

The PCA procedure eliminates the principal components that contribute less than a prefixed percentage to the total variation in the data set (1% in the present paper). The remaining Principal Components (6 in this case) have to be selected. By projecting the training defect vectors on the 6 Principal Components, the training input matrix has been reduced from 46x100 to 6x100, with a very limited loss of information. Note that 46 are the significant features originally extracted by the previous feature extraction module, and 100 are the number of defect simulations. A further problem to manage is the exiguity of the defect simulations. In order to increase the training set, three further matrices have been generated from the original database. Each matrix element has been obtained by adding to the original matrix element a value randomly chosen in a range between -1% and 1% to take into account the noise. The new training input matrix, whose dimension is 6x400, has been built by joining the 4 matrices. The output matrix has been generated by repeating the original output matrix four times. Finally, these new matrices have been used to train a MLP neural network. One matrix column each seven has been extracted to form the test set which has 14 fault cases. The remaining columns have been used to form the training and the validation sets.

### 3.5 Neural Networks

As previously noted, the neural network structure depends on the number of input features, namely

on the data reduction method. The number of input neurons is imposed by the features selection procedure; the number of output neurons is imposed by the code of the predicted values, while the number of hidden neurons has to be experimentally determined.

The following MLP architecture has been used, in case of PCA:

- Six 6 input nodes corresponding to the 6 selected principal components;
- One hidden layer with 40 nodes and hyperbolic tangent (tansig in matlab) as activation function;
- Two output nodes corresponding to the dimension of the defect (width and depth), decimal coded. The output nodes activation function is linear.

The stopping criteria consist of a maximum number epochs equals to 500, and a minimum mean square error equal to 10E-5.

The training phase reached a mean square error equals to 4.09E-5 after 100 epochs. The defect position has not been considered in the neural network models because a preliminary analysis showed that this value could be determined by the knowledge of the return time of the reflected wave. In fact, the return time is linearly dependent only from the defect position, while it is not influenced by the other geometrical characteristics.

### 3.6 Results

After the training phase, the network performances have been tested with a test set composed by the 14 defect cases, which correspond to the configurations (position, width, and depth) listed in Table 4. The use of the PCA technique provides good classification accuracy. In Fig. 3 and 4 the percentage errors are shown versus the defect width, and depth respectively. The percentage errors of the neural network trained for the fault classification are always less than 7%. The smallest errors are related to faults faraway the transducer. In this case the received signal is almost free from the residual oscillation due to the applied force. The easiest parameter characterizing the faults to be classified is its width: the biggest percentage error is less than 5%.

In both cases, the performance of the neural network models for the fault classification is very encouraging, offering good classification accuracy.

Deleted: ,

Deleted: s

Deleted: 100

Deleted: epochs

Deleted: s

Deleted: MSE

Deleted: 500

Deleted: for

**Table 4: Test Set**

Conf.	Position[m]	Width[mm]	Depth[mm]
1	0.5	30	1
2	1	30	4
3	2	12	1
4	2.5	12	1
5	3	12	2
6	3	24	1
7	3	30	4
8	3.5	30	4
9	4.5	12	1
10	5	12	1
11	5	30	4
12	5.5	12	4
13	6.5	18	2
14	7	30	4

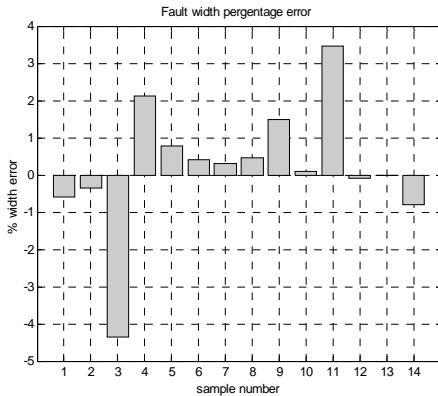


**Fig. 3. Neural Network fault width percentage errors on the 14 test set cases.**

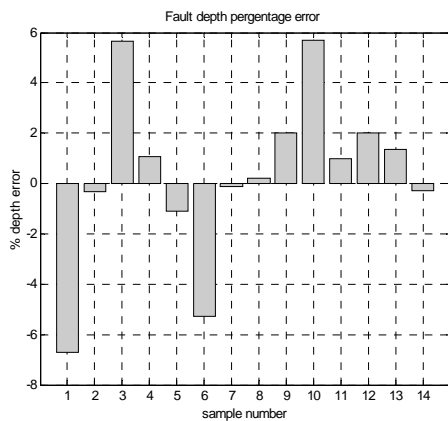


**Fig. 4. Neural Network fault depth percentage errors on the 14 test set cases.**

## 4 Torsional Wave Mode

The second type of signals has been provided by the research group of the University of Pisa and they have been simulated by the finite element code CAPA.

These signals have been obtained by building three-dimensional models of pipes with defects symmetric respect to the axis and by using a torsional mode as excitation. The dimensions and the geometric characteristics of the pipes are shown in Table 5.

The dimensions of the elements in the FEM model, and the sampling time are shown in Table 6.

**Table 5: Geometric dimensions and material properties of the modeled pipe**

<b>Length of the pipe</b>	2.1m
<b>Outer radius</b>	0.043 m
<b>Thickness</b>	0.0055 m
<b>Young's modulus</b>	219 GN/m <sup>2</sup>
<b>Poisson's coefficient</b>	0.286
<b>Density</b>	8000 kg/m <sup>3</sup>

**Table 6: Element dimensions and sampling time**

<b>Number of axial subdivisions</b>	1420
<b>Number of radial subdivisions</b>	1
<b>Number of circumferential subdivisions</b>	36
<b>Sampling time [ms]</b>	3.03 10 <sup>-4</sup>
<b>Excitation frequency [kHz]</b>	55

### 4.1 Fault diagnosis

The simulated defects have different depth and width and they are located at the same distance from the edge of the pipe, equal to 1.3 m.

For the fixed position, the notch width and depth have been varied as reported in Table 7.

The resulting data set is composed by 95 defect cases, which are divided in two sets: the training set is composed by 80 cases, while the test set is composed by 15 defect cases, which correspond to the configurations (depth and width) listed in Table 8.

The excitation signal is a six-cycle tone displacement enclosed in a Hanning window, applied at the extremity of the model.

The received waveforms represent the circumferential displacement of 36 equispaced

Deleted:

Deleted: Sampling

Deleted: signals

Deleted: 72

**Table 7: Geometric fault characteristics**

	Range	Step
Depth [mm]	0.55-4.95	1.1
Width [mm]	3-210	variable

**Table 8: Test set**

Depth [mm]	Width [mm]
0.55	63
0.55	123
0.55	210
1.65	60
1.65	120
1.65	180
2.75	45
2.75	105
2.75	165
3.85	30
3.85	90
3.85	150
4.95	15
4.95	75
4.95	135

points located in a section at a distance of 0.6 m from the edge of the pipe. Because of the axisymmetric defect model, the displacement in each node is the same. Therefore it is sufficient to consider just one signal for each defect to train the network.

**4.2 Data reduction**

For this new set of data, FFT and PCA have been sequentially applied to the temporal signals without extracting the previously mentioned features. The temporal signals have been firstly processed by FFT. Then PCA has been used to reduce the number of the inputs.

It has been demonstrated that the defect depth influences the FFT amplitude, while the defect width influences the shape of the waves, and, consequently, the FFT phase [8] [20]. Thus, PCA has been applied to the FFT amplitude components obtaining 8 inputs to be used to predict defect depths, with a loss of information of 1%. The PCA has been applied to the FFT phase components obtaining 4 inputs to be used to predict defect width, with a loss of information of 1%.

**4.3 Neural Networks**

The following MLP architecture has been used to predict the defect depth:

- Input: 8 input nodes;
- One hidden layer with 10 nodes and logarithmic sigmoid transfer function (logsig in matlab) as activation function;
- One output node corresponding to the dimension of the defect depth, decimal coded. The output node activation function is linear.

The stopping criteria consist of a maximum number equals to 300 epochs, and a minimum mean square error equal to 1.0E-4.

The training phase reached a mean square error equals to 4.7E-4 after 20 epochs.

The following MLP architecture has been used to predict the defect width:

- Input: 4 input nodes;
- One hidden layer with 10 nodes and logsig as activation function;
- One output node corresponding to the dimension of the defect width, decimal coded. The output node activation function is linear.

The stopping criteria consist of a maximum number of epochs equal to 300, and a minimum mean square error equal to 1.0E-4.

The training phase reached a mean square error equals to 9.5E-5 after 20 epochs.

**4.4 Results**

The network performances have been tested on the test set in Table 8.

In particular, the percentage errors of the neural network trained for the depth fault classification are less than 6.1%, with an average error of 5.4%.

The percentage errors of the neural network trained for the width fault classification are less than 5.9%, with an average error of 1.5%.

Also for torsional mode excitation, the performance of the neural network models for the fault classification is very encouraging, offering good classification accuracy.

**5 Conclusions**

A diagnostic system based on Neural Networks for Non-Destructive Testing with ultrasonic waves in not accessible pipes has been implemented. The signal database for the training, validation and test set has been obtained by using the finite element method. The signals are preprocessed with DWT, Blind Separation, FFT, and PCA techniques to obtain input data suitable to be fed to neural networks.

Deleted: F  
Deleted: C

Deleted: s

Deleted: s

Deleted: MSE

Deleted: s

Deleted: s

Deleted: epochs

Deleted: s

Deleted: MSE

Deleted: ¶

Formatted: Bullets and Numbering

Formatted: Bullets and Numbering

Deleted: based on Neural Networks



Two kinds of excitation have been examined: Longitudinal wave mode and Torsional wave mode.

The preliminary analyses of the numerically simulated defects, shows that the return time of the reflected signal linearly depends on the defect position, while it is independent on the entity of the fault. The flaw position is therefore determined with precision only from the knowledge of this value.

Although the obtained results are encouraging, this paper represents only a preliminary contribution in testing the neural network suitability to perform non-destructive defect detection. In fact, the training, validation and test sets have been synthetically generated by numerically simulating the defects.

Recently, the present research received a grant by the Italian Ministry for Research, to realize a real diagnostic system. The research is carried out by five research groups from Italian universities and it is coordinated by University of Pisa.

Future work will be devoted to improve the neural network performances and to test them with data measured on real pipes by means of an instrumentation that has been recently purchased by the University of Pisa.

### Acknowledgement

The authors would like to thank Francesco Bertoncini and Marco Raugi for providing data.

The work was supported by the grant PRIN 2003 of the MIUR (Italian Ministry for Research).

### References:

[1] M. J. S. Lowe, D.N. Alleyne, and P. Cawley, Defect detection in pipe using guided waves, *Ultrasonics*, Vol. 36, 1988, pp. 147-154.

[2] D. N. Alleyne, B. Pavlakovi, M. J. S. Lowe, and P. Cawley, Rapid Long range Inspection of Chemical Plant Pipework Using Guided Waves, *Proc. of the World Conference of NDT*, Rome, 15-20 Oct., 2000.

[3] P. Cawley, and D. N. Alleyne, The use of lamb waves for the Long-Range Inspection of large structures, *Ultrasonics*, Vol. 34, 1996, pp. 287-290.

[4] R. O. Duda, and P. E. Hart, *Pattern classification and Scene Analysis*, John Wiley & Sons, 1973.

[5] L. Reinhold, and W. Lord, A finite-element formulation for the study of Ultrasonic NDT Systems, *IEEE Trans. on Ultrasonics*,

*Ferroelectrics and Frequency Control*, Vol. 35, 1998, pp. 809-820.

[6] M: H: S. Siqueira, C: E: N: Gatts, R: R Silva, and J. M. A. Rebello, The use of ultrasonic guided waves and wavelets analysis in pipe inspection, *Ultrasonics*, Vol. 41, 2004, pp. 785-797.

[7] A. Hyvarinen, and J. Hurri, Blind separation of sources that have spatiotemporal variance dependencies, *Signal Processing*, Vol. 84, 2004, pp. 247-254.

[8] A. Demma, P. Cawley, and M. Lowe, The reflection of the fundamental torsional mode from cracks and notches in pipes, *J.Acoustic. Soc. Am.* Vol. 114, 2003, pp. 611-625.

[9] *CAPA WisSoft*, Buckenhof, Germany-Release: 4.1

[10] A. Fanni, A. Giua, M. Marchesi, and M. Montisci, A neural network diagnosis approach for analog circuits, *Applied Intelligence*, Kluwer Academic Pub., Vol. 11, 1999, pp. 169-186.

[11] *Ansys Release Note*, Version 8.1, 2003.

[12] J. Barshinger, J. L. Rose, and M.J. Jr. Avioli, Guided Wave Resonance Tuning for Pipe Inspection, *Journal of Pressure Vessel Technology*, Vol. 124, 2002, pp. 303-310.

[13] F. Moser, L. J. Jacobs, and J. Qu, Modeling elastic wave propagation in waveguides with the finite element method, *NDT&E int.*, Vol. 32, 1999, pp 225-234.

[14] O. C. Zienkiewicz, A new look at Newmark, Houbolt and other time-stepping formulae: A weighted residual approach, *Eathquake Eng Strct. Dyn.*, Vol. 5, 1977, pp. 413.

[15] L. B. Jackson, *Digital Filters and Signal Processing*, 1995.

[16] C. H. Chen, Application of Wavelet Transform to Ultrasonic NDE and Remote-Sensing Signal Analysis, *IEEE*, Vol. 8, 1994.

[17] A. Cichocki and S. Amari, *Adaptive Blind Signal and Image Processing Learning Algorithms and Applications*, Wiley&Sons, 2003.

[18] *Signal Processing Toolbox for MATLAB R12*, 2004.

[19] T. J. Case, and R. C. Waag, Flaw identification from time and frequency features of ultrasonic waveforms, *IEEE Trans. on Ultrasonics and Frequency Control*, Vol. 43, 1996, pp. 592-600.

[20] A. Oppenheim, and Jae S. Lim, The importance of the phase in Signals, *Proc. of the IEEE*, Vol. 69, 1981, pp. 529-541.

Deleted: have

Deleted: shown

Deleted: from

Deleted: from